

Collision processes of CH_y and CH_y^+ hydrocarbons with plasma electrons and protons

R. K. Janev and D. Reiter^{a)}

Institut für Plasmaphysik, Forschungszentrum-Jülich GmbH, EURATOM Association, Trilateral Euregio Cluster, D-52425 Jülich, Germany

(Received 21 January 2002; accepted 24 May 2002)

The critical fusion reactor design issue of tritium codeposition in tokamaks with carbon as wall material is closely linked with the plasma chemistry involving hydrocarbons. A complete set of cross sections for all important electron- and proton-impact processes with CH_y ($y=1-4$) hydrocarbon impurities and their ions CH_y^+ is presented. The cross sections are derived on the basis of most recent experimental information and well established cross section scaling relationships. The cross sections are presented in closed analytic forms convenient for implementation in plasma simulation codes. © 2002 American Institute of Physics. [DOI: 10.1063/1.1500735]

I. INTRODUCTION

The presence of hydrocarbon impurities in fusion edge plasmas (and, in particular, divertors) may significantly influence the properties and dynamic behavior of these plasmas through their cooling (radiative and dissociative) potential,¹ fuel dilution, and their plasma recombination capabilities.² The hydrocarbon fragmentation dynamics is an important ingredient of their transport in edge plasmas,^{3,4} in the studies of their radiation properties⁵ and, most importantly, for the critical divertor design issue of tritium codeposition. If this problem is not solved, then the leading candidate material, carbon, for ITER (International Thermonuclear Experimental Reactor) and future fusion reactors would be eliminated.

A quantitative understanding of tritium and carbon deposition in divertors of magnetic fusion devices is not available at present. Subcomponents of this problem are the unresolved issues of the carbon sources at the walls, the transport in the scrape-off-layer including, apparently, effects of large scale convection and, finally, the hydrocarbon chemistry- and neutral transport mechanisms.

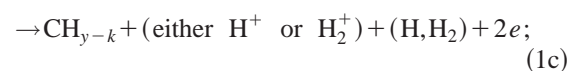
In this article we provide the atomic and molecular data necessary to separate this latter issue from the two former ones, computationally by plasma edge simulation, and, hence, to make these two better accessible to experimental investigation.

The computational task of solving the multidimensional and multi-species hydrocarbon transport and chemistry problem is largely in hand, due to availability of 3D Monte Carlo kinetic transport codes for fusion edge plasmas.⁶ Understanding (or quantitative modeling) of hydrocarbon transport or hydrocarbon radiative properties in fusion edge plasmas, or their effects on the behavior and/or properties of these plasmas, is, therefore, determined by the accuracy of the knowledge of the characteristics of their collision processes with plasma electrons and protons, such as rate coefficients

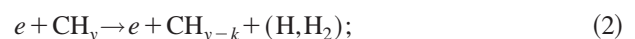
(or cross sections), energy and momentum redistribution during the collision, etc. Attempts to provide this information have been made in the past for the CH_y ($y=1-4$) family of hydrocarbons⁷ and for the heavier hydrocarbons, C_2H_y and C_3H_y .⁴ The widely used database in Ref. 7 has to be regarded as completely obsolete in view of the large amount of new experimental information on the corresponding processes and the improved understanding of the physical mechanisms governing these processes. Also the more recent database⁴ on collision processes of higher hydrocarbons, C_2H_y and C_3H_y , does not adequately reflect the available experimental cross section information for these molecules and, in its most part, is based on unjustified physical assumptions about the dynamics of processes for which the cross sections are “derived” (guessed). Much more accurate cross section collections have recently been completed for charge exchange processes of protons with C_xH_y ($x=1-3$; $1 \leq y \leq 2x+2$)⁸ and electron-impact ionization of C_xH_y ($x=1-3$; $1 \leq y \leq 2x+2$),⁹ based on the most recent experimental cross section information and on physically well justified and reliable cross section scaling relationships.

In the present article we give a complete cross section database for the most important collision processes of electrons and protons with CH_y ($y=1-4$) and CH_y^+ hydrocarbon species, supplemented by the energetics of all individual reaction channels for these processes. The processes included in the present database are:

electron-impact direct (I) and dissociative (DI) ionization of CH_y ,

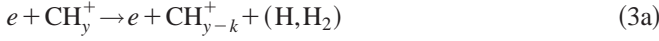


electron-impact dissociative excitation of CH_y to neutrals (DE),



^{a)} Author to whom correspondence should be addressed. Electronic mail: d.reiter@fz-juelich.de

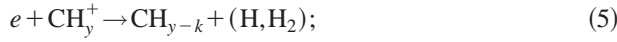
electron-impact dissociative excitation of CH_y^+ ions (DE),



electron-impact dissociative ionization of CH_y^+ ions (DI),



electron dissociative recombination with CH_y^+ ions (DR),



and proton-impact charge and atom exchange reactions (CX)



where in Eqs. (1b), (1c), and (2)–(5) all (important) fragmentation channels are supposed to be included. By the parentheses (H, H₂) we mean the appropriate number (if any) of neutral hydrogen atom or neutral hydrogen molecule reaction products in each of these channels.

The processes (4) of dissociative ionization of CH_y^+ ions are expected to be of less importance than processes (3a) and (3b), at least in the rather cold divertor plasmas, due to their large energy thresholds (≥ 25 eV). However, we include them in the present analysis for completeness, and because they may be relevant in low recycling limiter tokamaks and stellarators. The cross sections for the above processes are obtained either from the most recent experimental data or on the basis of established scaling relationships.^{8,9} In the following sections we briefly discuss each of these types of processes, with emphasis on the way of determining the corresponding cross sections. The cross sections are presented by analytic expressions having proper physical behavior at both low and high collision energies. In the energy regions where experimental data are available for a given process, these analytic cross section expressions represent a least-square-fit of the data.

II. ELECTRON IMPACT IONIZATION OF CH_y (I AND DI)

Very accurate ($\sim 10\%$) partial cross sections for the direct and six dissociative electron-impact ionization channels for the CH_4 molecule have become available recently from two experimental groups.^{10,11} Experimental data of similar accuracy have been recently reported also for the direct ($\text{CH}_y \rightarrow \text{CH}_y^+ + e$) and the dominant dissociative ($\text{CH}_y \rightarrow \text{CH}_{y-1}^+ + \text{H} + e$) ionization channels of the $e + \text{CH}_y$ ($y = 1-3$) collision systems.¹² For the other important dissociative channels of CH_y ($y = 1-3$) molecules, the corresponding cross sections were derived in Ref. 9 by using the additivity rules for the strengths of chemical bonds. Table I shows all important ionization channels in $e + \text{CH}_y$ ($y = 1-4$) collisions. The ionization (or appearance) potentials (threshold energies) for all these channels are also given in Table I (taken from Ref. 13), together with the mean energy

TABLE I. Ionization (I_p)/ appearance (A_p) potentials (from Ref. 13) and reaction energetics for ionization channels of CH_y ($y = 1-4$) (from Ref. 14).

Reaction	I_p or A_p (eV)	$\bar{E}_{\text{el}}^{(-)}$ (eV)	\bar{E}_K (diss. products) (eV)	
$e + \text{CH}_4$	$\rightarrow \text{CH}_4^+ + 2e$	12.63	12.63	...
	$\rightarrow \text{CH}_3^+ + \text{H} + 2e$	14.25	17.49	3.2
	$\rightarrow \text{CH}_2^+ + \text{H}_2 + 2e$	15.1	18.83	3.7
	$\rightarrow \text{CH}^+ + \text{H}_2 + \text{H} + 2e$	19.9	23.5	3.6
	$\rightarrow \text{C}^+ + 2\text{H}_2 + 2e$	19.6	24.6	5.0
	$\rightarrow \text{H}^+ + \text{CH}_3 + 2e$	18.0	20.7	3.0
	$\rightarrow \text{H}_2^+ + \text{CH}_2 + 2e$	20.1	25.6	6.0
$e + \text{CH}_3$	$\rightarrow \text{CH}_3^+ + 2e$	9.84	9.84	...
	$\rightarrow \text{CH}_2^+ + \text{H} + 2e$	15.12	20.4	5.3
	$\rightarrow \text{CH}^+ + \text{H}_2 + 2e$	15.74	21.64	6.0
	$\rightarrow \text{C}^+ + \text{H}_2 + \text{H} + 2e$	19.50	28.84	8.0
	$\rightarrow \text{H}^+ + \text{CH}_2 + 2e$	18.42	24.8	7.5
	$\rightarrow \text{H}_2^+ + \text{CH} + 2e$	20.18	28.2	6.0
$e + \text{CH}_2$	$\rightarrow \text{CH}_2^+ + 2e$	10.40	10.40	...
	$\rightarrow \text{CH}^+ + \text{H} + 2e$	15.53	20.4	5.0
	$\rightarrow \text{C}^+ + \text{H}_2 + 2e$	14.67	21.4	6.5
	$\rightarrow \text{H}^+ + \text{CH} + 2e$	18.01	23.4	6.4
	$\rightarrow \text{H}_2^+ + \text{C} + 2e$	18.83	25.5	6.5
$e + \text{CH}$	$\rightarrow \text{CH}^+ + 2e$	11.13	11.13	...
	$\rightarrow \text{C}^+ + \text{H} + 2e$	14.74	18.35	4.31
	$\rightarrow \text{H}^+ + \text{C} + 2e$	17.07	23.0	5.94

loss of the incident electron $\bar{E}_{\text{el}}^{(-)}$ and total kinetic energy of reaction products \bar{E}_K , (taken from Ref. 14). The energy \bar{E}_K is distributed among the products according to

$$\bar{E}_j = \frac{\mu}{M_j} \bar{E}_K. \quad (7)$$

Here M_j is the mass of product j , and μ is the reduced mass of the products.

The cross sections σ_I and σ_{DI} of reaction channels listed in Table I can all be represented by analytic fit functions of the form

$$\sigma = \frac{10^{-13}}{EI_c} \left[A_1 \ln \left(\frac{E}{I_c} \right) + \sum_{j=2}^N A_j \left(1 - \frac{I_c}{E} \right)^{j-1} \right] (\text{cm}^2), \quad (8)$$

where E is the collision energy (in eV), I_c is a parameter close (or equal) to the appearance potential (expressed in eV), and A_j ($j = 1, \dots, N$) are fitting coefficients. The number N of these parameters was chosen to ensure a rms deviation of the fit better than 2%–3%. The values of fitting parameters I_c and A_j for all reactions in Table I are given in the Appendix. The total ionization cross sections for CH_y ($y = 1-4$) molecules have also been fitted by Eq. (8) and the corresponding coefficients I_c and A_j are also given in the Appendix.

We also note that the total electron-impact ionization cross sections

$$\sigma_{I+DI}^{\text{tot}} := \sigma_I + \sigma_{DI}^{\text{tot}}$$

for CH_y molecules can be represented by a single analytic expression of the parameter y (accurate to within 10%–20%)

$$\sigma_{I+DI}^{\text{tot}}(\text{CH}_y) = 84.0(1 + 0.373y) \left(1 - \frac{I_p}{E}\right)^3 \frac{1}{E} \times \ln(e + 0.09E) (\times 10^{-16} \text{ cm}^2), \quad (9)$$

where I_p is the ionization potential of CH_y (in eV), $e = 2.71828 \dots$, and y is the number of H atoms in CH_y. [The collision energy E in Eq. (9) is also expressed in units of eV.] The linearity of $\sigma_{I+DI}^{\text{tot}}(\text{CH}_y)$ on y is a direct manifestation of the above mentioned additivity rules. Similar linearities on y show also the partial cross sections for same reaction products.⁹ This is a result of the energy invariance of reaction branching ratios, observed for energies above ≈ 30 eV.^{9,15}

III. DISSOCIATIVE EXCITATION OF CH_y TO NEUTRALS (DE)

There are no direct experimental measurements or theoretical calculations of dissociative excitation of CH_y molecules ($y = 1-4$) to neutral products [reaction (2)]. The cross section measurements for CH₃ and CH₂ radical production in $e + \text{CH}_4$ collisions reported in Ref. 16 are not consistent with the accurate measurements of Refs. 10 and 11 for the two ion production channels $\text{CH}_4 \rightarrow \text{CH}_3 + \text{H}^+ + e$ and $\text{CH}_4 \rightarrow \text{CH}_2 + \text{H}_2^+$ which contain the same radicals. Therefore, we adopt the approach (followed also in Ref. 7) to represent the total cross section σ_{DE}^{tot} as difference of the *total* dissociation cross section for a CH_y molecule, σ_D^{tot} and the total dissociative ionization cross section σ_{DI}^{tot} , i.e.,

$$\sigma_{DE}^{\text{tot}}(\text{CH}_y) = \sigma_D^{\text{tot}}(\text{CH}_y) - \sigma_{DI}^{\text{tot}}(\text{CH}_y). \quad (10)$$

While $\sigma_{DI}^{\text{tot}}(\text{CH}_y)$ is known for all CH_y ($y = 1-4$) molecules (see preceding section and the Appendix), $\sigma_D^{\text{tot}}(\text{CH}_y)$ is known only for CH₄.¹⁷

By virtue of the additivity rules for the strengths of chemical bonds one can expect that the total cross sections $\sigma_{DE}^{\text{tot}}(\text{CH}_y)$ and $\sigma_{I+DI}^{\text{tot}}(\text{CH}_y)$ are proportional to each other. Knowing the ratio $\sigma_{DE}^{\text{tot}}/\sigma_{I+DI}^{\text{tot}}$ for CH₄, one can then determine the total cross sections σ_{DE}^{tot} for all other CH_y ($y = 1-3$) molecules, at least for $E \geq 30$ eV where the additivity rules are strictly valid. For energies below ~ 30 eV, the magnitude of $\sigma_{DE}^{\text{tot}}(\text{CH}_y)$ are determined by its threshold behavior $(1 - E_{\text{th}}/E)^\alpha$, with $\alpha \approx 3$.

For determining the cross sections of different neutral dissociation channels, one needs to invoke the fact that the dissociation of CH_y to neutrals and the dissociative ionization of CH_y are governed by a common physical mechanism: excitation of a dissociative state which lies in the ionization continuum.^{18,19} Autoionization of this state leads to dissociative ionization, while its survival leads to dissociation to neutrals. On this basis one should expect that the contribution R_{DI} of dissociative ionization channel $\text{CH}_y \rightarrow \text{A}^+ + \dots + e$ to $\sigma_{DI}^{\text{tot}}(\text{CH}_y)$, and the contribution R_{DE} of dissociative channel $\text{CH}_y \rightarrow \text{A} + \dots$ to $\sigma_{DE}^{\text{tot}}(\text{CH}_y)$ are equal, i.e.,

$$\frac{\sigma_{DE}(A/\text{CH}_y)}{\sigma_{DE}^{\text{tot}}(\text{CH}_y)} = R_{DE}(A) = R_{DI}(A^+) = \frac{\sigma_{DI}(A^+/\text{CH}_y)}{\sigma_{DI}^{\text{tot}}(\text{CH}_y)}. \quad (11)$$

TABLE II. Neutral dissociative channels of CH_y: branching ratios, R_{DE} , threshold energies, E_{th} (from Ref. 13), mean electron energy loss, $\bar{E}_{\text{el}}^{(-)}$, and mean total kinetic energy of products, \bar{E}_K (from Ref. 14).

Reaction	Channel	R_{DE}	$E_{\text{th}} = \bar{E}_{\text{el}}^{(-)}$ (eV)	\bar{E}_K (products) (eV)
$e + \text{CH}_4$	$\rightarrow \text{CH}_3 + \text{H} + e$	0.760	8.8	4.4
	$\rightarrow \text{CH}_2 + \text{H}_2 + e$	0.144	9.4	4.7
	$\rightarrow \text{CH} + \text{H}_2 + \text{H} + e$	0.073	12.5	4.5
	$\rightarrow \text{C} + 2\text{H}_2 + e$	0.023	14.0	6.0
$e + \text{CH}_3$	$\rightarrow \text{CH}_2 + \text{H} + e$	0.83	9.5	4.7
	$\rightarrow \text{CH} + \text{H}_2 + e$	0.14	10.0	5.5
	$\rightarrow \text{C} + \text{H}_2 + \text{H} + e$	0.03	15.0	7.0
$e + \text{CH}_2$	$\rightarrow \text{CH} + \text{H} + e$	0.90	8.5	4.25
	$\rightarrow \text{C} + \text{H}_2 + e$	0.08	8.2	4.9
	$\rightarrow \text{C} + 2\text{H} + e$	0.02	14.0	6.2
$e + \text{CH}$	$\rightarrow \text{C} + \text{H} + e$	1.0	7.0	3.5

Here we have introduced the notation $\sigma(A/B)$ for the cross section of a collision process $B + \dots \rightarrow A + \dots$.

The neutral dissociative channels of CH_y molecules are shown in Table II together with their branching ratios R_{DE} . This table also gives the mean energy loss $\bar{E}_{\text{el}}^{(-)}$ of the incident electrons (equal to the reaction threshold energy), and the mean total kinetic energy of the products, \bar{E}_K (taken from Ref. 14). It should be noted that for $E \geq 30$ eV the branching ratios R_{DE} do not depend on the energy,⁹ while for $E < 30$ eV the behavior of the cross section $\sigma_{DE}(A)$ is fully determined by the position of the threshold. The total cross sections $\sigma_{DE}^{\text{tot}}(\text{CH}_y)$ for all CH_y ($y = 1-4$) molecules, the determination of which was described earlier, can be represented by a single function

$$\sigma_{DE}^{\text{tot}}(\text{CH}_y) = 34.6(1 + 0.29y) \left(1 - \frac{E_{\text{th}}}{E}\right)^3 \frac{1}{E} \times \ln(e + 0.15E) (\times 10^{-16} \text{ cm}^2), \quad (12)$$

where y is the number of H atoms in CH_y, the collision and threshold energies (E and E_{th}) are expressed in eV, and $e = 2.71828 \dots$. The partial cross section for a particular neutral dissociation channel $\text{CH}_y \rightarrow \text{A} + \text{B}$ is now given by

$$\sigma_{DE}(A/\text{CH}_y) = R_{DE}(A/\text{CH}_y) \sigma_{DE}^{\text{tot}}(\text{CH}_y), \quad (13)$$

where the values of branching ratios $R_{DE}(A/\text{CH}_y)$ are given in Table II.

Here, as well as in the tables below for the other reaction types, the branching ratios R_k for the various channels k are given independent of the collision energy E . A possible refinement of this, accounting for the distinct threshold energies $E_{\text{th},k}$ of these individual channels, is given by the reduction formula:

$$\tilde{R}_k(E) = 0 \quad \text{for } E < E_{\text{th},k}$$

and

$$\tilde{R}_k(E) = \frac{R_k}{1 - (1 - R_k) \left(\frac{E_{\text{th},k}}{E} \right)^2} - \sum_{j=1}^{k-1} \tilde{R}_j(E_{\text{th},k})$$

for $E \geq E_{\text{th},k}$.

The indexing k and j of the channels in this formula, for any particular process DE, DI, DR, etc., has to be such that the channels are ordered with increasing threshold energy $E_{\text{th},k}$. Furthermore, these modified energy dependent branching ratios have to be renormalized, for each energy, so that their sum over k becomes 1.

IV. DISSOCIATIVE EXCITATION (DE) OF CH_y^+ BY ELECTRON IMPACT

Total cross section measurements for the electron-impact dissociative excitation of CH_y^+ ions, reactions (3a) and (3b), have not been performed so far. However, experimental cross section data have become available recently for the H^+ and H_2^+ ion production channels in electron collisions with CH_y^+ ions ($y=1-5$),^{20,21} for the C^+ -production channel in $e + \text{CH}^+$ collisions,²² and for the H^+ production channel in $e + \text{CH}_2^+$ collisions.²³

The measured H^+ -, H_2^+ - and C^+ -production cross section contain contributions from both DE and dissociative ionization DI processes. Thus, the H^+ production cross section in $e + \text{CH}^+$ collisions is the sum of the cross sections for $\text{C} + \text{H}^+$ (DE) and $\text{C}^+ + \text{H}^+ + e$ (DI) channels. Similarly, the C^+ -production cross section in $e + \text{CH}^+$ collisions (measured in Ref. 22) is the sum of the cross sections for $\text{C}^+ + \text{H}$ (DE) and $\text{C}^+ + \text{H}^+ + e$ (DI) channels. For the $e + \text{CH}^+$ system, the cross section for the DE channel $\text{C} + \text{H}^+$ has been measured independently (in storage ring experiments²⁴), thus allowing us to separate the contribution of the DI channel in the H^+ production cross section for this collision system.

As we will see later, the separation of DE and DI contributions in the H^+ - and H_2^+ -production cross sections is possible also for other CH_y^+ ions.

A. Capture auto-ionization dissociation (CAD) versus “proper” DE

It is important to note that the CH_y^+ dissociation (without ionization) may proceed via two mechanisms: a direct mechanism, corresponding to the excitation of a dissociative state of CH_y^+ (by “vertical” transition from the ground state of CH_y^+), and a capture-auto-ionization mechanism, corresponding to capture of an incident electron on a doubly excited dissociative Rydberg state CH_y^{**} of the CH_y molecule, the auto-ionization of which leads to dissociation of CH_y^+ . Both mechanisms produce the same reaction products. (The survival of the doubly excited dissociative state against auto-ionization contributes to the dissociative recombination of CH_y^+ ions, see Sec. VI.)

Only the first of these two mechanisms is a proper DE-process. The capture-auto-ionization dissociation (CAD) mechanism is an “indirect” process and requires the existence of “core-excited” states of CH_y^+ with the same disso-

TABLE III. Dissociative excitation channels of CH_y^+ : branching ratios, R_{DE}^+ , threshold energies, E_{th} (from Ref. 13), mean electron energy loss, $\bar{E}_{\text{el}}^{(-)}$, and mean total kinetic energy of products, \bar{E}_K (from Ref. 14).

Reaction	Channel	R_{DE}^+	$E_{\text{th}} = \bar{E}_{\text{el}}^{(-)}$ (eV)	\bar{E}_K (products) (eV)
$e + \text{CH}_4^+$	$\rightarrow \text{CH}_3^+ + \text{H} + e$	0.360	5.2	3.6
	$\rightarrow \text{CH}_3 + \text{H}^+ + e$	0.315	8.0(#)	2.6
	$\rightarrow \text{CH}_2^+ + \text{H}_2 + e$	0.140	6.5	4.0
	$\rightarrow \text{CH}_2 + \text{H}_2^+ + e$	0.073	9.5(#)	2.0
	$\rightarrow \text{CH}^+ + \text{H}_2 + \text{H} + e$	0.068	10.0	2.4
	$\rightarrow \text{C}^+ + 2\text{H}_2 + e$	0.044	10.4	3.7
$e + \text{CH}_3^+$	$\rightarrow \text{CH}_2^+ + \text{H} + e$	0.256	10.6	5.3
	$\rightarrow \text{CH}_2 + \text{H}^+ + e$	0.515	11.0 ^a	2.5
	$\rightarrow \text{CH}^+ + \text{H}_2 + e$	0.125	12.0	6.1
	$\rightarrow \text{CH} + \text{H}_2^+ + e$	0.048	11.3 ^a	0.8
	$\rightarrow \text{C}^+ + \text{H}_2 + \text{H} + e$	0.056	14.0	4.5
$e + \text{CH}_2^+$	$\rightarrow \text{CH}^+ + \text{H} + e$	0.195	12.0	7.0
	$\rightarrow \text{CH} + \text{H}^+ + e$	0.675	9.0 ^a	2.4
	$\rightarrow \text{C} + \text{H} + \text{H}^+ + e$	0.040	14.2	3.3
	$\rightarrow \text{C}^+ + \text{H}_2 + e$	0.056	11.0	6.8
	$\rightarrow \text{C} + \text{H}_2^+ + e$	0.021	11.6 ^a	3.3
	$\rightarrow \text{C}^+ + 2\text{H} + e$	0.013	15.5	6.8
$e + \text{CH}^+$	$\rightarrow \text{C}^+ + \text{H} + e$	0.09	12.2 ^b	8.2
	$\rightarrow (\text{CH})^{**} \rightarrow \text{C}^+ + \text{H} + e$	1.0	2.5	4.0
	$\rightarrow \text{C} + \text{H}^+ + e$	0.91	5.0 ^a	2.0

$\bar{E}_{\text{el}}^{(-)} = 8.4^b$

^aExperimental threshold energies, Refs. 20 and 21.

^bObtained from potential energy curves of CH^+ (Ref. 25).

ciation limit. The CAD process exhibits a much smaller threshold energy than the DE process. Thus, the “vertical” (DE) threshold for this channel is about 5.0 eV.²⁰ This indicates that the observed H^+ -production cross section contains also a (relatively small) contribution from the CAD process. In contrast to this, the “vertical” (DE) threshold for the $\text{C}^+ + \text{H}$ dissociation of CH^+ is ≈ 12.2 eV,²⁵ while the experimental threshold for this channel is ≈ 2.5 eV.²² This means that the observed experimental cross section for C^+ -production, at least in the energy range below the $\text{C}^+ + \text{H}^+ + e$ reaction threshold (≈ 29.0 eV²⁵), is almost entirely due to the CAD process. The contribution of the direct DE process to the $\text{C}^+ + \text{H}$ dissociation channel in the energy range above ~ 12.2 eV can be estimated from the threshold energy behavior of direct DE processes [see Eq. (14)]. For the cross section ratio of $\text{C}^+ + \text{H}$ and $\text{H}^+ + \text{C}$ DE channels of CH^+ dissociation this gives $(5/12.2)^{2.5} \approx 0.11$, i.e., $\sigma_{DE}(\text{C}^+/\text{CH}^+)$ contributes about 10% to $\sigma_{DE}^{\text{tot}}(\text{CH}^+)$ in the energy region sufficiently far from both thresholds.

B. The direct (“proper”) DE processes

Next we discuss the cross sections $\sigma_{DE}(\text{CH}_y^+)$ for the direct electron-impact dissociative reactions of CH_y^+ ions.

Using the similarity of electron impact dissociative excitation processes of CH_y and CH_y^+ systems, one can adopt (in accordance with the additivity rules) that the increase of total dissociative excitation cross section $\sigma_{DE}^{\text{tot}}(\text{CH}_y^+)$ of CH_y^+ ions with increasing the number y of its H constituents is the same as that of $\sigma_{DE}^{\text{tot}}(\text{CH}_y)$, at least in the energy range above

~20–30 eV. With the known value of the $\sigma_{DE}^{\text{tot}}(\text{CH}^+)$ cross section [obtained as sum of the experimental $\sigma_{DE}(\text{H}^+/\text{CH}^+)$ cross section^{20,22} and the above estimated 10% contribution of $\sigma_{DE}(\text{C}^+/\text{CH}^+)$ to $\sigma_{DE}^{\text{tot}}(\text{CH}^+)$], one can then determine $\sigma_{DE}^{\text{tot}}(\text{CH}_y^+)$ for all other CH_y⁺ ($y=2-4$) molecular ions.

Using the known cross sections for the H⁺ and H₂⁺ production cross sections in dissociative ionization for all CH_y⁺ ions considered here, the values of $\sigma_{DE}^{\text{tot}}(\text{CH}_y^+)$, and the linear dependence of fractional contributions $R_{DE}^+(A^+/\text{CH}_y^+)$ of the channels $\text{CH}_y^+ \rightarrow A^+ + \dots$ to $\sigma_{DE}^{\text{tot}}(\text{CH}_y^+)$ on y , one can derive the values of branching ratios $R_{DE}^+(A^+/\text{CH}_y^+)$ for all dissociative excitation channels of CH_y⁺ ions.¹⁴ The values of R_{DE}^+ for the various dissociative excitation channels of CH_y⁺ are given in Table III. In this table are also given the threshold energies (E_{th}), the mean electron energy loss ($\bar{E}_{\text{el}}^{(-)} = E_{\text{th}}$), and the mean total kinetic energy of dissociated products (\bar{E}_K) for all dissociative excitation channels of CH_y⁺ ions (taken from Ref. 14).

The total dissociative excitation cross section $\sigma_{DE}^{\text{tot}}(\text{CH}_y^+)$ for all CH_y⁺ ions can be represented by a single analytic fit function

$$\begin{aligned} \sigma_{DE}^{\text{tot}}(\text{CH}_y^+) &= 29.4[1 + 0.71(y-1)] \\ &\times \left(1 - \frac{E_{\text{th}}}{E}\right)^{2.5} \frac{1}{E} \\ &\times \ln(e + 0.9E) \quad (\times 10^{-16} \text{cm}^2), \end{aligned} \quad (14)$$

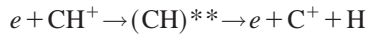
where collision and threshold energies (E and E_{th}) are expressed in units of eV, and $e = 2.71828 \dots$. The partial cross sections for individual dissociative excitation channels $\text{CH}_y^+ \rightarrow A^+ + \dots$ are then given by

$$\sigma_{DE}(A^+/\text{CH}_y^+) = R_{DE}^+(A^+/\text{CH}_y^+) \sigma_{DE}^{\text{tot}}(\text{CH}_y^+), \quad (15)$$

with R_{DE}^+ (as well as E_{th}) given in Table III.

C. The CAD processes

The cross section for the capture-auto-ionization dissociation process



can be obtained from the experimental data of Ref. 22 on the C⁺-ion production cross section by subtracting the contribution to this cross section coming from the DI channel $\text{C}^+ + \text{H}^+ + e$ in the energy region above 29.0 eV (the threshold of this DI channel). This subtraction was done in such a way that the energy dependence of $\sigma_{CAD}(\text{C}^+/\text{CH}^+)$ in the energy region above $\approx 35-40$ eV is the same as the energy dependence of $\sigma_{DE}(\text{C}^+/\text{CH}_y^+)$ cross section. The obtained $\sigma_{CAD}(\text{C}^+/\text{CH}^+)$ cross section can be represented by the analytic fit expression

$$\begin{aligned} \sigma_{CAD}(\text{C}^+/\text{CH}^+) &= 20.6 \left(1 - \frac{E_{\text{th}}}{E}\right)^{2.5} \frac{1}{E} \\ &\times \ln(e + 0.9E) \quad (\times 10^{-16} \text{cm}^2), \end{aligned} \quad (16)$$

where $E_{\text{th}} = 2.5$ eV. From the potential curves of dissociative states of CH⁺ ion converging to the $\text{C}^+ + \text{H}$ dissociation limit,²⁵ one can estimate the total kinetic energy of the C⁺

+H products to be ≈ 4.0 eV. (The E_{th} and \bar{E}_K values for this process are also given in Table III.) The closeness of observed energy thresholds of H⁺- and H₂⁺-DE channels of CH_y⁺ ($y=2-4$) ions with those which can be calculated from thermochemical tables¹³ (see also Ref. 14) indicates that the CAD contribution to the H⁺- and H₂⁺-ion production is negligible. However, with regard to the CAD contribution to C⁺-ion production dissociative channels for these ions listed in Table III, in the absence of any experimental cross section information, or potential energy calculations of excited CH_y⁺ ($y=2-4$) states, it is difficult to make an estimate of corresponding CAD cross sections. The resonant structures observed in the dissociative recombination cross sections of these ions (see next section) in the energy region above 1–2 eV can be taken as an indication that the CAD mechanism contributes to the C⁺-ion dissociation channels in these collision systems. The magnitude of this contribution, however, cannot be estimated at present.

V. DISSOCIATIVE IONIZATION (DI) OF CH_y⁺ BY ELECTRON IMPACT

We now discuss the cross sections σ_{DI} for dissociative ionization of CH_y⁺ ions [reaction (4)]. As we mentioned at the beginning of the preceding section, the total DI cross section for CH_y⁺ ions can be derived as difference between the experimental H⁺-ion production cross section for this ion²⁰ and independently measured cross section for the $\text{C} + \text{H}^+$ dissociative excitation.²⁴ This procedure determines $\sigma_{DI}^{\text{tot}}(\text{CH}^+)$ up to $E = 70$ eV. There are also theoretical calculations for this cross section,²⁶ which agree with $\sigma_{DI}^{\text{tot}}(\text{CH}^+)$ derived from the experiments, and extend the cross section into the KeV region. $\sigma_{DI}^{\text{tot}}(\text{CH}^+)$ has a maximum at about 80–100 eV.

The main reaction channels of dissociative electron-impact ionization of CH_y⁺ ions are given in Table IV. All of these are H⁺-ion production channels. Therefore, the total DI cross section for a given CH_y⁺ ion is $\sigma_{DI}^{\text{tot}}(\text{CH}_y^+) \approx \sigma_{DI}(\text{H}^+/\text{CH}_y^+)$ and can be determined from the total experimental H⁺-ion production cross section^{20,21} by subtracting from it the partial $\sigma_{DE}(\text{H}^+/\text{CH}_y^+)$ cross section, given by Eq. (14) and the $R_{DE}^+(\text{H}^+)$ value from Table III. The cross sections $\sigma_{DI}^{\text{tot}}(\text{CH}_y^+)$ obtained in this way up to $E = 70$ eV [the last experimental energy for the $\sigma_{DE}(\text{H}^+/\text{CH}_y^+) + \sigma_{DI}(\text{H}^+/\text{CH}_y^+)$ sum] can be extended to higher energies by assuming that the ratios $\sigma_{DI}(\text{H}^+/\text{CH}_y^+)/\sigma_{DI}^{\text{tot}}(\text{H}^+/\text{CH}^+)$ remain the same as their values in the energy range 40–70 eV (in which these ratios are essentially energy independent). Knowing $\sigma_{DI}^{\text{tot}}(\text{H}^+/\text{CH}^+)$ in the entire energy range and the above ratios for each CH_y⁺ ion, the total DI cross sections $\sigma_{DI}^{\text{tot}}(\text{CH}_y^+) \approx \sigma_{DI}(\text{H}^+/\text{CH}_y^+)$ for all CH_y⁺ ions can be represented by the analytic fit function

$$\begin{aligned} \sigma_{DI}^{\text{tot}}(\text{CH}_y^+) &= 30.1[1 + 0.086(y-1)] \\ &\times \left(1 - \frac{E_{\text{th}}}{E}\right)^{1.55} \frac{1}{E} \\ &\times \ln(e + 0.5E) (\times 10^{-16} \text{cm}^2). \end{aligned} \quad (17)$$

TABLE IV. Main reaction channels in dissociative ionization of CH_y^+ : branching ratios, R_{DI}^+ , threshold energies, E_{th} (from Ref. 13), mean electron energy loss, $\bar{E}_{el}^{(-)}$ ($=E_{th}$), and mean total kinetic energy of ionic products, $\bar{E}_K(\text{ion.prod.})$ [$\bar{E}_K(\text{neutr.prod.})=0$].

Reaction	Channel	R_{DI}^+	$E_{th}=\bar{E}_{el}^{(-)}$ (eV)	\bar{E}_K (ion.prod.) (eV)
$e + \text{CH}_4^+$	$\rightarrow e + \text{CH}_3^+ + \text{H}^+ + e$	0.35	27.05	11.78
	$\rightarrow e + \text{CH}_2^+ + \text{H} + \text{H}^+ + e$	0.24	32.48	11.78
	$\rightarrow e + \text{CH}^+ + \text{H}_2 + \text{H}^+ + e$	0.22	33.09	11.78
	$\rightarrow e + \text{C}^+ + \text{H}_2 + \text{H} + \text{H}^+ + e$	0.19	36.76	11.78
$e + \text{CH}_3^+$	$\rightarrow e + \text{CH}_2^+ + \text{H}^+ + e$	0.40	30.81	11.78
	$\rightarrow e + \text{CH}^+ + \text{H} + \text{H}^+ + e$	0.31	35.94	11.78
	$\rightarrow e + \text{C}^+ + \text{H}_2 + \text{H}^+ + e$	0.29	35.09	11.78
$e + \text{CH}_2^+$	$\rightarrow e + \text{CH}^+ + \text{H}^+ + e$	0.55	30.41	11.78
	$\rightarrow e + \text{C}^+ + \text{H} + \text{H}^+ + e$	0.45	34.15	11.78
$e + \text{CH}^+$	$\rightarrow e + \text{C}^+ + \text{H}^+ + e$	1.00	29.0	11.78

In the region below ~ 40 eV, the cross section behavior is dominantly determined by the threshold factor $(1 - E_{th}/E)^{1.55}$. We see that $\sigma_{DI}^{\text{tot}}(\text{CH}_y^+)$ has a rather weak linear dependence on y .

The DI reaction channels not included in Table IV contain CH_k^+ and H_2^+ reaction products. Their cross sections can, in principle, be determined by subtracting $\sigma_{DE}(\text{H}_2^+/\text{CH}_y^+)$ from the experimentally known H_2^+ -ion production cross sections, $\sigma_{DE}(\text{H}_2^+/\text{CH}_y^+) + \sigma_{DI}(\text{H}_2^+/\text{CH}_y^+)$.²¹ However, the H_2^+ -ion production cross sections are about an order of magnitude smaller than the H^+ -ion production cross sections.²¹ Moreover, the thresholds of H_2^+ DI channels are always larger than the thresholds of H^+ DI channels, which further reduces their cross sections with respect to those of the H^+ DI channels.

The threshold energies in Table IV for DI channels were determined in the following way:

For the CH^+ ion, the “vertical” energy to reach the $(\text{C}^+ + \text{H}^+)$ potential energy curve from the energy minimum of CH^+ ground electronic state is 29.0 eV.²⁵ It lies 11.78 eV above the $(\text{C}^+ + \text{H}^+)$ dissociation limit (infinite internuclear distances). The amount of 11.78 eV is the Coulomb interaction energy of C^+ and H^+ ions after the Franck–Condon transition from the CH^+ ground electronic state to $(\text{C}^+ + \text{H}^+)$ dissociating state is accomplished. This (interaction) energy depends on the ion charges only and has been added to the calculated dissociation energies (using thermochemical tables, Ref. 13) of all DI channels in Table IV. The charged reaction products share the amount of 11.78 eV according to Eq. (7). The neutral products in DI channels of Table IV have zero kinetic energy.

As in the case of other types of reactions considered in the present article, one can expect that the branching ratios $R_{DI}(A^+/\text{CH}_y^+)$ for individual DI reaction channels producing $A^+ + \text{H}^+$ ionic products in a $e + \text{CH}_y^+$ collision should be energy invariant for energies well above the threshold. Therefore, for $E \geq 50$ –60 eV, the partial DI cross sections for a given CH_y^+ ion can be expressed as

TABLE V. Values of fitting parameters in Eq. (19) for dissociative recombination in $e + \text{CH}_y^+$ systems.

Collision system	A	a	α	β
$e + \text{CH}_4^+$	3.0	0.1	1.25	1
$e + \text{CH}_3^+$	4.8	0.8	1.10	0.5
$e + \text{CH}_2^+$	6.7	1.2	1.15	0.5
$e + \text{CH}^+$	3.16	0.13	0.75	1.0

$$\sigma_{DI}(A^+/\text{CH}_y^+) = R_{DI}^+(A^+/\text{CH}_y^+) \sigma_{DI}^{\text{tot}}(\text{CH}_y^+). \quad (18)$$

There is, however, no experimental basis to determine the branching ratios R_{DI}^+ . In the absence of such information, we shall determine $R_{DI}^+(A^+/\text{CH}_y^+)$ from the threshold behavior of $\sigma_{DI}^{\text{tot}}(A^+/\text{CH}_y^+)$, which is $\propto [(E - E_{th})/E]^\alpha \approx (E - E_{th})^\alpha / E_{th}^\alpha$ when $E \rightarrow E_{th}$. Assuming that any two $R_{DI}^+(A_1^+/\text{CH}_y^+)$ and $R_{DI}^+(A_2^+/\text{CH}_y^+)$ branching ratios have the same energy dependence (if any) in the regions near the thresholds of $A_1^+ + \text{H}^+$ and $A_2^+ + \text{H}^+$ channels, respectively, one finds

$$R_{DI}^+(A_1^+/\text{CH}_y^+) / R_{DI}^+(A_2^+/\text{CH}_y^+) \approx \left(\frac{E_{th2}}{E_{th1}} \right)^\alpha,$$

where $\alpha = 1.55$ [see Eq. (17)]. By using such ratios and the condition that the sum of all $R_{DI}^+(A_i^+/\text{CH}_y^+)$ should be one, we have determined the R_{DI}^+ values given in Table IV. Under the assumption made in their derivation (equal energy dependence of R_{DI}^+ in the threshold region) the extension of obtained R_{DI}^+ values to high energies is justified.

VI. DISSOCIATIVE RECOMBINATION (DR) OF ELECTRONS WITH CH_y^+

Total cross section measurements for the dissociative recombination of electrons with CH_y^+ ($y=1-5$) have been performed in both merged beams²⁷ and storage ring experiments.^{23,28-30} It appeared that due to a calibration error, the data reported in Ref. 28, used in the database,⁷ are by a factor of 2 too large.³¹ The present database uses the most

TABLE VI. Dissociation channels in $e + \text{CH}_y^+$ recombination: branching ratios, R_{DR} , and total kinetic energy, $E_K^{(0)}$ of products (in their ground states and for $E_{el}=0$, from Ref. 14).

Reaction	Channel	R_{DR}	$E_K^{(0)}$ (eV)
$e + \text{CH}_4^+$	$\rightarrow \text{CH}_3 + \text{H}$	0.21	8.17
	$\rightarrow \text{CH}_2 + \text{H}_2$	0.09	7.83
	$\rightarrow \text{CH}_2 + \text{H} + \text{H}$	0.43	3.30
	$\rightarrow \text{CH} + \text{H}_2 + \text{H}$	0.25	3.42
	$\rightarrow \text{C} + \text{H}_2 + \text{H}_2$	0.02	4.43
$e + \text{CH}_3^+$	$\rightarrow \text{CH}_2 + \text{H}$	0.40	4.97
	$\rightarrow \text{CH} + \text{H}_2$	0.14	5.10
	$\rightarrow \text{CH} + \text{H} + \text{H}$	0.16	0.64
	$\rightarrow \text{C} + \text{H}_2 + \text{H}$	0.30	1.57
$e + \text{CH}_2^+$	$\rightarrow \text{CH} + \text{H}$	0.25	6.0
	$\rightarrow \text{C} + \text{H}_2$	0.12	7.00
	$\rightarrow \text{C} + \text{H} + \text{H}$	0.63	2.47
$e + \text{CH}^+$	$\rightarrow \text{C} + \text{H}$	1.0	7.18

recent storage-ring data for CH_y⁺ ($y=1-3$),^{23,28,29} given in the energy range $\sim 10^{-4}$ –20 eV, and only for CH₄⁺ it uses the corrected data of Ref. 27 (given in the energy range $\sim 10^{-3}$ –4 eV). In the energy region above ~ 1 –2 eV, the total recombination cross sections $\sigma_{DR}^{\text{tot}}(\text{CH}_y^+)$ show resonant structures, pronounced particularly in the energy region around 5–10 eV where the thresholds of competing dissociative excitation processes lie (see Table III). After averaging over these resonances, the cross sections $\sigma_{DR}^{\text{tot}}(\text{CH}_y^+)$ ($y=1-4$) can all be represented in the form

$$\sigma_{DR}^{\text{tot}}(\text{CH}_y^+) = \frac{A}{E^\alpha(1+aE)^\beta} \quad (\times 10^{-16} \text{cm}^2), \quad (19)$$

where the fitting parameters A , α , a and β are given in Table V and E is expressed in eV units. The value of parameters α is close (or equal) to one, in accordance with the Wigner's law for break-up reactions. In Refs. 23, 29, and 30 the branching ratios R_{DR} of different dissociative recombination channels have been measured for CH₂⁺, CH₃⁺ and CH₅⁺ ions, respectively. The branching ratios for CH_y⁺ ions ($y=1-4$) are given in Table VI, where the values of R_{DR} for CH₄⁺ are obtained by interpolation between corresponding ratios for the CH₃⁺ and CH₅⁺ ions. Table VI also gives the total kinetic energy $E_K^{(0)}$ of the dissociated products for a zero electron impact energy and when the products are in their ground state.¹⁴ If the electron impact energy in the center-of mass system is E , the total kinetic energy of dissociated product is $E_K = E + E_K^{(0)}$. The products from the dissociative recombination process, however, are most probably excited, which follows from the nature of the main (direct) mechanism for this process (electron capture to a doubly excited repulsive state of the CH_y molecule). Because of the large excitation energy of H atoms, and in view of the experimental evidence for the case of CH⁺ ion,²⁸ it is most probable that for $E \lesssim 10$ eV only the CH_y ($y=0-3$) recombination products are in excited states. The experimental evidence with the $e + \text{CH}^+$ recombination²⁸ indicates that the lowest excited states of CH_y products are "core-excited" states, the excitation energies of which are relatively small (~ 1 –2 eV). For this amount the values of $E_K^{(0)}$ in Table VI should be reduced. [For instance, the $e + \text{CH}^+$ recombination below 9.0 eV leads to formation C(¹D) + H(1S) and C(¹S) + H(1s) fragments, the first channel having $R_{DR}=0.75$ and $E_K^{(0)}=5.92$ eV, while the second channel has $R_{DR}=0.25$ and $E_K^{(0)}=4.50$ eV.²⁸] Knowing the values of branching ratios R_{DR} , the cross sections for individual dissociative recombination channels $\text{CH}_y^+ \rightarrow A + B + \dots$ are given by

$$\sigma_{DR}(A/\text{CH}_y^+) = R_{DR}(A/\text{CH}_y^+) \sigma_{DR}^{\text{tot}}(\text{CH}_y^+). \quad (20)$$

VII. CHARGE EXCHANGE AND PARTICLE EXCHANGE PROCESSES

The cross section database for charge exchange (or charge transfer, or electron capture) processes (6a), as well as for particle exchange processes (6b), was discussed in detail in Ref. 8 together with the similar processes of higher hydrocarbons, C₂H_y and C₃H_y. Therefore we shall here describe only the main aspects and results for the CH_y ($y=1-4$)

TABLE VII. Charge exchange reaction channels in H⁺ + CH_y thermal collisions: Total thermal rate coefficients, K_{cx}^{tot} , branching ratios, R_{cx} , and reaction exothermicities, ΔE (from Ref. 14).

Reaction	Channel	K_{cx}^{tot} (10^{-9} cm ³ /s)	R_{cx}	ΔE (eV)
H ⁺ + CH ₄	→ H + CH ₄ ⁺	3.8	0.4	1.1 ^a
	→ H ₂ + CH ₃ ⁺ + e	3.8	0.6	2.96
H ⁺ + CH ₃	→ H + CH ₃ ⁺ + e	3.4	1.0	3.78 ^a
H ⁺ + CH ₂	→ H + CH ₂ ⁺ + e	2.8	0.36	3.2
	→ H ₂ + CH ⁺ + e	2.8	0.64	5.17
H ⁺ + CH	→ H + CH ⁺	1.9	0.31	2.47
	→ H ₂ + C ⁺	1.9	0.69	5.28

^aThese exothermicities are absorbed by reaction products.

family of hydrocarbons. We first note that the thermal rate coefficients K_{cx} for the sum of reactions (6a) and (6b) are known from astrophysical literature.³² This information, together with the estimated branching ratio $R_{cx}^{(a)}$, $R_{cx}^{(b)}$ (on the basis of exothermicities of these channels), can serve as a basis to determine the low-energy limit for the cross sections of reactions (6a) and (6b). Moreover, using the orbiting (polarization) mechanism for the charge and particle exchange reactions in the thermal energy range ($E \lesssim 0.05$ eV), the cross sections of reactions (6a) and (6b) can in this energy region be written as⁸

$$\sigma_{cx}^{(a)} = 7.26 \frac{R_{cx}^{(a)} K_{cx}^{\text{tot}}}{E^{1/2}} \quad (\times 10^{-16} \text{cm}^2), \quad (21)$$

$$\sigma_{cx}^{(b)} = 7.26 \frac{R_{cx}^{(b)} K_{cx}^{\text{tot}}}{E^{1/2} + cE^\gamma} \quad (\times 10^{-16} \text{cm}^2), \quad (22)$$

where the collision energy E is expressed in eV, $R_{cx}^{(a)}$ and $R_{cx}^{(b)}$ are the branching ratios of reactions (6a) and (6b) in the thermal energy region, and K_{cx}^{tot} is the total rate coefficient for both (6a) and (6b) channels expressed in units of 10^{-9} cm³/s. The second term in the denominator of Eq. (22) reflects the fact that the cross section of particle exchange reactions decreases faster than that for pure electron capture when the collision energy becomes larger than the typical thermal energies. The values of K_{cx}^{tot} , $R_{cx}^{(a),(b)}$ are given in Table VII, together with reaction exothermicities ΔE for each channel. (For H⁺ + CH₃, only the electron capture channel is exothermic.) The parameters c and γ are $c=0.5$ and $\gamma=2.5$ for the H⁺ + CH₄ and H⁺ + CH₂ reactions, respectively, and $c=0.01$ and $\gamma=3.5$ for the H⁺ + CH reaction.

The cross sections for these reactions have not been measured for collision energies above the thermal ones, except for the pure electron capture process in the H⁺ + CH₄ collision system. For this particular system, experimental cross sections are available from ~ 40 eV/amu up to the MeV/amu region.³³⁻³⁸ With the recent data for the O⁺ + CH₄ system,³⁹ which is electronically almost identical to the H⁺ + CH₄ system (H and O have almost identical ionization potentials), the collision energy range with available cross section data is extended down to 12 eV/amu. In this entire energy range, the electron capture cross section for H⁺ + CH₄ shows a typical resonant cross section behavior

TABLE VIII. Values of fitting parameters c_i in Eq. (23) for electron capture reactions.

c_i	$H^+ + CH_4$	$H^+ + CH_3$	$H^+ + CH_2$	$H^+ + CH$
c_1	3.93	17.0	7.32	4.28
c_2	445.0	385.0	0.005	0.001
c_3	2.3	2.5	3.0	3.0
c_4	46.2	51.3	20.95	20.2
c_5	0.00	0.00	1.55	5.3
c_6	0.57	0.35
c_7	0.094	0.096	0.00	0.00
c_8	9.0×10^{-6}	2.0×10^{-9}	2.35×10^{-7}	1.12×10^{-6}
c_9	1.2	2.0	1.55	1.45
c_{10}	2.845×10^{-18}	5.5×10^{-21}	5.86×10^{-21}	1.10×10^{-20}
c_{11}	3.8	4.3	4.26	4.3
c_{12}	5.81×10^{-22}	0.00	0.00	0.00
c_{13}	4.4

(logarithmic increase with decreasing the collision energy), and smoothly joins the cross section Eq. (21) in the thermal region. In Ref. 8 it was argued that the cross sections for $H^+ + CH_3$ system should have a similar resonant behavior. It was shown in Ref. 8 that the $H^+ + C_xH_y \rightarrow H + C_xH_y^+$ reactions with $y \geq 2x$ all have resonant character and on that basis a cross section scaling relation was revealed for these reactions in the collision energy region below ~ 20 keV/amu. The validity of another scaling law was demonstrated in Ref. 8 for all $H^+ + C_xH_y$ systems in the energy region above ~ 100 keV/amu. These two scaling laws were used in Ref. 8 (together with a plausible interpolation in the range 10–100 keV/amu) to determine the cross sections for the collision systems for which no experimental or theoretical cross section information is available in the literature. (For the systems $H^+ + C_xH_y$, with $y < 2x$, additional criteria were used for determination of σ_{cx} in the energy region below ~ 20 keV/amu.)

The derived cross sections for electron capture channel (6a) were analytically represented in Ref. 8 by analytic fit functions using Chebishev polynomials. In order to ensure correct cross section behavior outside the range of fitted data, we take here an analytic fit function of the form

$$\sigma_{cx}^{(a)} = \frac{c_1}{E^{0.5} + c_2 E^{c_3}} + \frac{c_4 \exp(-c_5/E^{c_6})}{E^{c_7} + c_8 E^{c_9} + c_{10} E^{c_{11}} + c_{12} E^{c_{13}}} \quad (\times 10^{-16} \text{cm}^2), \quad (23)$$

where E is the collision energy expressed in units of eV, and c_i are the fitting parameters. The values of c_i are given in Table VIII.

VIII. CONCLUDING REMARKS

We have presented a complete cross section database for all important collision processes of electrons and protons with hydrocarbon CH_y ($y = 1-4$) molecules and their ions for use in fusion applications (hydrocarbon transport modeling and diagnostics). In this database we have used the most recent experimental data and information regarding the mechanisms governing the considered reactions. In particular, semi-empirical cross section scaling relationships, originating from the stability of chemical bond strengths with respect to external perturbations,^{40,41} have been used for deriving the electron-impact reaction cross sections when such were not available in the literature. Similar scaling relationships were used in the derivation of charge exchange cross sections of CH_y ($y = 1-3$) with protons.

All cross sections are represented in form of analytic fit functions valid in a broad energy range (from threshold, or thermal energy region for exothermic reactions up to several keV for electron impact, and several hundred keV for proton impact reactions). For dissociative processes, all important dissociative channels have been included in the database.

The accuracy of presented cross sections for electron-impact processes is within 10%–15%, when the cross sections are obtained from experimental sources, and 15%–30% when they are derived from scaling relationships. The charge exchange cross section for CH_4 is believed to be accurate to within 15%–20%, while for the other molecules the cross section accuracy is lower ($\sim 30\%$ – 40% for energies below ~ 1 eV and above 1 keV, and even higher for the energies in the range 1 eV to 1 keV). The average energy lost by the reactants and/or gained by the reaction products is provided for each of the considered reactions. Because the energies of excited (dissociative) states of CH_y molecules and CH_y^+ ions are known only for CH and CH^+ , the estimated average energy loss/gain values for electron-impact processes for other systems may have an uncertainty of 1–2 eV.

APPENDIX: FITTING COEFFICIENTS FOR IONIZATION CROSS SECTIONS

Values of the fitting coefficients in Eq. (8) for the total and partial ionization cross sections in $e + CH_y$ collisions. For each process I_c and A_i (i from 1 to N) are listed. $5.1090E+02$ means 5.1090×10^2 .

$e + CH$

(a) Total cross section

Process	I_c	$A_i, i=1,3$	$A_i, i=4,6$	$A_i, i=7,8$
$e + CH \rightarrow$ total ionization	1.1200E+01	1.2258E+00	-3.0764E+00	2.6182E+01
		-1.4891E+02	4.3224E+02	-6.6387E+02
		5.1090E+02	-1.5314E+02	

(b) Partial cross sections

Process	I_c	$A_i, i=1,3$		
		$A_i, i=4,6$		
$e + \text{CH} \rightarrow \text{CH}^+ + 2e$	1.1300E+01	1.4439E+00	-1.2724E+00	-2.2221E+00
		9.2822E+00	-1.5506E+01	8.2778E+00
$e + \text{CH} \rightarrow \text{C}^+ + \text{H} + 2e$	1.4800E+01	4.3045E-01	-4.1305E-01	-5.6881E-01
		3.2957E+00	-5.6549E+00	3.4295E+00
$e + \text{CH} \rightarrow \text{C} + \text{H}^+ + 2e$	1.7140E+01	4.4144E-02	-1.8579E-02	-4.1046E-01
		2.3115E+00	-4.1040E+00	2.7436E+00

 $e + \text{CH}_2$ **(a) Total ionization**

Process	I_c	$A_i, i=1,3$		
		$A_i, i=4,6$		
$e + \text{CH}_2 \rightarrow \text{total ionization}$	1.0910E+01	2.9597E+00	-2.6451E+00	-3.7136E+00
		8.9168E+00	-1.2872E+01	5.8594E+00

(b) Partial cross sections

Process	I_c	$A_i, i=1,3$		
		$A_i, i=4,6$		
$e + \text{CH}_2 \rightarrow \text{CH}_2^+ + 2e$	1.0400E+01	1.7159E+00	-1.7164E+00	-6.5529E-01
		2.1724E+00	-5.4186E+00	3.1616E+00
$e + \text{CH}_2 \rightarrow \text{CH}^+ + \text{H} + 2e$	1.5530E+01	8.1919E-01	-7.5016E-01	-3.8063E-03
		1.4065E+00	-3.6447E+00	2.6220E+00
$e + \text{CH}_2 \rightarrow \text{C}^+ + \text{H}_2 + 2e$	1.7100E+01	3.8400E-02	-2.91786E-02	-0.98490E-01
		0.73008E+00	-1.2111E+00	0.85722E+00
$e + \text{CH}_2 \rightarrow \text{CH} + \text{H}^+ + 2e$	2.2300E+01	-5.8168E-02	8.2064E-02	5.2048E-02
		3.1915E-01	-1.3363E-01	2.3477E-01
$e + \text{CH}_2 \rightarrow \text{C} + \text{H}_2^+ + 2e$	2.4800E+01	2.7682E-02	5.0215E-02	3.7494E-04
		5.1300E-01	-6.1525E-01	6.2835E-01

 $e + \text{CH}_3$ **(a) Total cross section**

Process	I_c	$A_i, i=1,3$		
		$A_i, i=4,6$		
$e + \text{CH}_3 \rightarrow \text{total ionization}$	9.8400E+00	2.4221E+00	-2.4368E+00	-7.4454E-01
		4.6634E-01	-4.1606E+00	4.5799E+00

(b) Partial cross sections

Process	I_c	$A_i, i=1,3$		
		$A_i, i=4,6$		
$e + \text{CH}_3 \rightarrow \text{CH}_3^+ + 2e$	9.8000E+00	1.9725E+00	-2.1011E+00	1.0593E+00
		-6.3438E+00	8.0140E+00	-4.2440E+00
$e + \text{CH}_3 \rightarrow \text{CH}_2^+ + \text{H} + 2e$	1.4000E+01	1.2824E+00	-1.3906E+00	6.2993E-01
		9.4521E-01	-5.3629E+00	4.3087E+00
$e + \text{CH}_3 \rightarrow \text{CH}^+ + \text{H}_2 + 2e$	1.6000E+01	1.1666E-01	-1.1254E-01	1.5594E-01
		-7.3177E-02	-2.1307E-01	5.5290E-01
$e + \text{CH}_3 \rightarrow \text{CH}_2 + \text{H}^+ + 2e$	1.8480E+01	-2.1667E-02	3.2699E-02	-1.3308E-01
		1.1473E+00	-1.9437E+00	1.5827E+00
$e + \text{CH}_3 \rightarrow \text{C}^+ + \text{H}_2 + \text{H} + 2e$	1.9540E+01	-9.5279E-03	1.7251E-02	-5.1275E-02
		4.0755E-01	-6.5843E-01	5.1835E-01
$e + \text{CH}_3 \rightarrow \text{CH} + \text{H}_2^+ + 2e$	2.0180E+01	-4.4067E-03	8.6072E-03	-2.0148E-02
		1.6728E-01	-2.6542E-01	2.1110E-01

$e + \text{CH}_4$ **(a) Total cross section**

Process	I_c	$A_i, i=1,3$	$A_i, i=4,6$	
$e + \text{CH}_4 \rightarrow \text{total ionization}$	1.2630E+01	2.3449E+00	-2.6163E+00	2.1843E-01
		1.0890E+01	-2.9718E+01	2.4582E+01

(b) Partial cross sections

Process	I_c	$A_i, i=1,3$	$A_i, i=4,6$	
$e + \text{CH}_4 \rightarrow \text{CH}_4^+ + 2e$	1.2630E+01	1.3541E+00	-1.4665E+00	1.6787E-01
$e + \text{CH}_4 \rightarrow \text{CH}_3^+ + \text{H} + 2e$	1.4010E+01	6.1801E+00	-1.5638E+01	1.0767E+01
$e + \text{CH}_4 \rightarrow \text{CH}_2^+ + \text{H}_2 + 2e$	1.6200E+01	1.6074E+00	-1.4713E+00	-2.7386E-01
$e + \text{CH}_4 \rightarrow \text{CH}^+ + \text{H}_2 + \text{H} + 2e$	1.6200E+01	1.9556E-01	1.1343E-01	9.0166E-03
$e + \text{CH}_4 \rightarrow \text{C}^+ + 2\text{H}_2 + 2e$	2.2200E+01	1.6252E-01	-1.0708E-01	-3.2252E-01
$e + \text{CH}_4 \rightarrow \text{CH}_2 + \text{H}_2^+ + 2e$	2.2300E+01	8.7125E-01	-1.8747E-02	1.3071E-01
$e + \text{CH}_4 \rightarrow \text{CH}_3 + \text{H}^+ + 2e$	2.1100E+01	-1.2458E-01	1.6287E-01	-3.3395E-01
		3.5738E+00	-5.0472E+00	2.8240E+00
		-2.2989E-01	7.7426E-01	-2.9020E-01
		-1.7615E-02	1.8347E-02	-5.0664E-02
		2.6118E-01	1.5316E-01	-1.7314E-01
		-3.4698E-01	-1.6026E-02	4.3296E+00
		-1.5155E+01	2.4766E+01	-1.0873E+01

¹U. Samm, H. L. Bay, P. Bogen *et al.*, Plasma Phys. Controlled Fusion **29**, 1321 (1987).

²R. K. Janev, T. Kato, and J. G. Wang, Phys. Plasmas **7**, 4364 (2000).

³W. D. Langer, Nucl. Fusion **22**, 751 (1982).

⁴D. A. Alman, D. N. Ruzic, and J. N. Brooks, Phys. Plasmas **7**, 1421 (2000).

⁵A. Huber, V. Philipps, A. Pospieszczyk *et al.*, J. Nucl. Mater. **290-293**, 276 (2001).

⁶D. Reiter, in *Atomic and Plasma-Material Interaction Processes in Controlled Thermonuclear Fusion*, edited by R. K. Janev and H. W. Drawin (Elsevier Science, Amsterdam, 1993), p. 243.

⁷A. B. Ehrhardt and W. D. Langer, "Collisional processes of hydrocarbons in hydrogen plasmas," Report PPPL-2477, Princeton Plasma Physics Laboratory, Princeton, NJ (Sept., 1987). See National Technical Information Service Department No. DE88003462. Copies may be ordered from The National Technical Information Service, Springfield, VA.

⁸R. K. Janev, J. G. Wang, and T. Kato, "Cross sections and rate coefficients for charge exchange reactions of protons with hydrocarbon molecules," Report NIFS-DATA-64 (May, 2001) (National Institute for Fusion Science, Toki, Japan), ISSN 0915-6364. Copies may be ordered from The Research Information Center, National Institute for Fusion Science, Oroshi, Toki, Gifu, 509-5292, Japan.

⁹R. K. Janev, J. G. Wang, I. Murakami, and T. Kato, "Cross section and rate coefficients for electron-impact ionization of hydrocarbon molecules," Report NIFS-DATA-68 (Oct. 2001) (National Institute for Fusion Science, Toki, Japan), ISSN 0915-6364. Copies may be ordered from The Research Information Center, National Institute for Fusion Science, Oroshi, Toki, Gifu, 509-5292, Japan.

¹⁰H. Straub, D. Lin, B. G. Lindsey, K. A. Smith, and R. F. Stebbings, J. Chem. Phys. **106**, 4430 (1997).

¹¹C. Tian and C. R. Vidal, J. Phys. B **31**, 895 (1998).

¹²V. Tarnovsky, A. Levin, H. Deutsch, and K. Becker, J. Phys. B **29**, 139 (1996).

¹³H. M. Rosenstock, K. Draxl, B. M. Steiner, and J. T. Herron, J. Phys. Chem. Ref. Data **6**(Suppl. 1), 1 (1977).

¹⁴R. K. Janev and D. Reiter, "Collision processes of hydrocarbon species in hydrogen plasmas: I. The methane family," Report FZ-Jülich Jül 3966 Feb. 2002 (Forschungszentrum-Jülich, Jülich, Germany), ISSN 0944-2952. Copies may be ordered from Forschungszentrum Jülich GmbH, Zentralbibliothek, D 52435 Jülich, Bundesrepublik Deutschland.

ntzialbibliothek, D 52435 Jülich, Bundesrepublik Deutschland.

¹⁵C. E. Melton, J. Chem. Phys. **37**, 562 (1962).

¹⁶T. Nakano, H. Toyoda, and H. Sugai, Jpn. J. Appl. Phys., Part 1 **30**, 2912 (1991).

¹⁷H. F. Winters, J. Chem. Phys. **63**, 3462 (1975).

¹⁸R. L. Platzman, Radiat. Res. **17**, 419 (1962).

¹⁹D. A. Vroom and F. J. de Heer, J. Chem. Phys. **50**, 573 (1969).

²⁰N. Djuric, Y. S. Chung, B. Wallbang, and G. H. Dunn, Phys. Rev. A **56**, 2887 (1997).

²¹N. Djuric, S. Zhou, G. H. Dunn, and M. E. Bannister, Phys. Rev. A **58**, 304 (1998).

²²Z. Amitay, D. Zajfman, P. Forck, U. Hechtischer, M. Grieser, D. Habs, D. Schwalm, and A. Wolf, in *Proceeding, 14th Conference on the Applications of Accelerators in Research and Industry*, Denton, 1996, AIP Conf. Proc. **392**, 51 (1997).

²³Å. Larson, A. Le Padellec, J. Semanyak *et al.*, Astrophys. J. **505**, 459 (1998).

²⁴P. Forck, Ph.D. thesis, Ruprecht-Karls-Universität Heidelberg, 1994, Cross section quoted in Ref. 20.

²⁵S. Green, P. S. Bagus, B. Liu, A. D. McLean, and M. Yoshimine, Phys. Rev. A **5**, 1614 (1972).

²⁶Y.-K. Kim, K. K. Irikura, and M. A. Ali, J. Res. Natl. Inst. Stand. Technol. **105**, 285 (2000).

²⁷P. M. Mul, J. B. A. Mitchell, V. S. D'Angelo, J. W. McGowan, and H. R. Froehlich, J. Phys. B **14**, 1353 (1981).

²⁸Z. Amitay, D. Zajfman, P. Forck, U. Hechtischer, B. Seidel, M. Grieser, D. Habs, R. Repnow, D. Schwalm, and A. Wolf, Phys. Rev. A **54**, 4032 (1996).

²⁹L. Vejby-Christensen, L. H. Andersen, O. Heber, D. Kella, H. B. Pedersen, H. T. Schmidt, and D. Zajfman, Astrophys. J. **483**, 531 (1997).

³⁰J. Semaniak, Å. Larson, A. Le Padellec *et al.*, Astrophys. J. **498**, 886 (1998).

³¹J. B. A. Mitchell, Phys. Rep. **186**, 215 (1990).

³²T. J. Millar, P. R. A. Facquhar, and K. Willacy, Astron. Astrophys., Suppl. Ser. **121**, 139 (1997).

³³M. L. Jones, B. Dougherty, and M. Dillingham, Nucl. Instrum. Methods Phys. Res. B **10/11**, 142 (1985).

³⁴J. G. Collins and P. J. Kebarle, J. Chem. Phys. **46**, 1082 (1967).

- ³⁵M. Elliot, *J. Phys. (France)* **38**, 24 (1977).
- ³⁶L. H. Taburen, Y. Nakai, and R. A. Langley, *Phys. Rev.* **171**, 114 (1968).
- ³⁷S. L. Varghese, G. Bissinger, M. J. Joyce, and R. Laubert, *Nucl. Instrum. Methods* **170**, 269 (1980).
- ³⁸T. Kusakabe, K. Asahina, A. Iida, Y. Tanaka, Y. Li, G. Hirsch, R. J. Buenker, M. Kimura, H. Tawara, and Y. Nakai, *Phys. Rev. A* **62**, 062715 (2000).
- ³⁹T. Kusakabe, R. Buenker, and M. Kimura, *At. Plasma-Mater. Interact. Data for Fusion* **10**, 151 (2002).
- ⁴⁰S. W. Benson and J. H. Buss, *J. Chem. Phys.* **29**, 546 (1958).
- ⁴¹D. R. Bates, *Int. J. Mass Spectrom. Ion Processes* **8**, 1 (1987).